RSC Advances

PAPER

View Article Online
View Journal | View Issue

Cite this: *RSC Adv.*, 2018, **8**, 35946

A dipodal molecular probe for naked eye detection of trivalent cations (Al^{3+}, $Fe^{3+}$and Cr^{3+}) in aqueous medium and its applications in real sample analysis and molecular logic gates†

Rukmani Chandra, Amit Kumar Manna, Kalyani Rout, Jahangir Mondal and Goutam K. Patra *

Received 22nd August 2018
Accepted 14th October 2018

DOI: 10.1039/c8ra07041e

rsc.li/rsc-advances

A simple and low cost multifunctional colorimetric receptor **L** has been designed, synthesized and characterized by ^{1}H-NMR, IR spectroscopy, ESI-MS spectrometry and elemental analysis. The chemosensor **L** can selectively detect three biologically and environmentally important trivalent metal ions (Al^{3+}, $Fe^{3+}$and Cr^{3+}) both visually and spectrophotometrically in CH_3CN–H_2O (1 : 1, v/v) solution in the presence of other biologically relevant metal ions. The Job's plot analyses indicate the 2 : 2 binding stereochemistry for Al^{3+}, Fe^{3+} and Cr^{3+} ions with **L**, which was further confirmed by ^{1}H-NMR and ESI-MS studies. The binding constant values were found to be 2.9×10^4 M^{-1} for Al^{3+}, 1.079×10^5 M^{-1} for Fe^{3+} and 1.366×10^5 M^{-1} for Cr^{3+} respectively. The detections limits of the sensor for Al^{3+} (2.8×10^{-7} M), Fe^{3+} (1.9×10^{-7} M) and Cr^{3+} (2.5×10^{-7} M) are far below than the limit set by the World Health Organization (WHO) for drinking water. Moreover, colorimetric test kits for rapid detection of Al^{3+}, Fe^{3+}, and Cr^{3+} could be successively applied for all practical purposes, indicating its potential use in environmental samples. It has also been used in building molecular logic gates.

Introduction

In recent years, colorimetric and fluorescent chemosensors have been recognized as powerful tools for naked eye detection of specific metal ions due to their high selectivity and sensitivity. Among various metal ions, trivalent cations have been a subject of intense research interest in the modern sensing arena because of their significant application in environment and biological systems.[1] The Al^{3+} ion, existing widely in the environment, can enter the human body through food and water.[2,3] Furthermore, aluminium toxicity is responsible for about 40% of the world's acidic soil.[4–6] On the other hand, aluminum compounds are not only used in industrial fields such as aluminum-based pharmaceuticals, food additives, medicines, water purification and production of light alloys but also used in our daily life as electronic and electrical compounds in different gadgets, building materials, packaging items *etc.*[7] High concentrations of Al^{3+} are harmful to plant growth and also to the human nervous system which further leads to lots of diseases such as microcytic hypochromic anemia, encephalopathy, myopathy, Alzheimer's disease, Parkinson's disease, amyotrophic lateral sclerosis *etc.*[8,9] As a result of the close relationship between aluminum and human health, the investigation on Al^{3+} detection attracts more and more attention. Secondly chromium, one of the most abundant elements in the earth's crust and sea water, exists as metallic (Cr^0), trivalent (Cr^{3+}), and hexavalent (Cr^{6+}) forms. Cr^{3+} is an essential element required for the proper functioning of biological processes. A recent study revealed that soluble Cr^{3+} between pH 6 to 8 can be found transiently in significant concentrations and has an undesirable effect on microorganism.[10] It acts as a glucose tolerance factor in some biochemical processes such as metabolism of carbohydrates, fats, proteins and nucleic acids by activating certain enzymes, stabilizing proteins and nucleic acids.[11] Chromium deficiency may influence the metabolism of glucose and lipids and lead to a variety of diseases, including diabetes and cardiovascular disease.[12] On the other hand, Fe^{3+} plays vital role in many physiological and pathological processes including cellular metabolism, enzyme catalysis and oxygen transport as well as DNA and RNA synthesis. The deficiency of iron in the human body lead to variety of diseases, including Parkinson's, anemia, diabetes, cancer and liver damage.[13] Therefore detection of Fe^{3+} is also required to a large extent.

Although, a number of analytical methods available for detections of Al^{3+}, $Fe^{3+}$and Cr^{3+}, including chromatography, accelerator mass spectroscopy (AMS), graphite furnace

Department of Chemistry, Guru Ghasidas Vishwavidyalaya, Bilaspur, CG, India. E-mail: patra29in@yahoo.co.in; Tel: +91 7587312992

† Electronic supplementary information (ESI) available. See DOI: 10.1039/c8ra07041e

atomic absorbance spectrometry (GFAAS), neutron activation analysis (NAA), inductively coupled plasma-atomic emission spectrometry (ICP-AES), inductively coupled plasma-mass spectrometry (ICP-MS), later ablation microprobe mass analysis (LAMMA) and electro thermal atomic absorption spectrometry (ETAAS)[14–18] but most of them require sophisticated instruments and time consuming and laborious procedures for sample preparation and in some cases expensive too. Consequently, spectro-photometric methods such as absorption and emission have become popular for sensing cations due to their high selectivity and sensitivity, low cost and real time monitoring. In addition, the detection of multiple analytes with a single receptor would be more efficient, which can also decrease the cost compared to one-to-one analysis method, and therefore would attract more attention.[19] Therefore, it is an urgent need to develop chemical sensors that are capable of detecting the presence of Al^{3+}, Fe^{3+} and Cr^{3+} ions in environmental and biological samples.

Schiff bases with *o*-substituted aromatic rings have found to be most responsive for chelation with transition metal ions. The chelation of transition metal ions to the >C=N linkage would develop ICT (intramolecular charge transfer) transition or make LMCT (ligand to metal charge transfer) transition, which could be useful for the visual sensing of the metal ions.[20] In this regard, 4-(diethylamino)-2-hydroxybenzaldehyde is a well-known chromophore used in the area of chemosensors. In continuation with our previous earlier research work,[21] we report here a chemosensor **L**, based on the combination of 4-(diethylamino)-2-hydroxybenzaldehyde and 4-(4-aminobenzyl)benzenamine for simultaneous detection of Al^{3+}, $Fe^{3+}$and Cr^{3+} ions by naked eye in CH_3CN–H_2O (1 : 1, v/v) mixture. For designing Schiff base we have selected amine part using two aniline moieties joined through a methylene rotor at their *para* positions and aldehyde part containing strong electron donating diethylamino group also in *para* position to the aldehyde, which makes it electron rich. **L** showed obvious color changes from colorless to yellow upon selective binding with Al^{3+}, Fe^{3+} and Cr^{3+} along with noticeable change in absorbance properties.

Experimental section

General information and materials

All of the materials used for synthesis were obtained from Sigma-Aldrich and used without further purification. All the solvents used were of analytical grade. Freshly de-ionized water was used throughout the experiment. The stock solutions of metal ions were prepared from their nitrate salts and the solutions of anions were prepared from their sodium salts. Elemental analysis was carried out on Elemental Vario MICRO cube analyzer. ^{1}H NMR spectra were recorded on a Bruker DRX spectrometer operating at 400 MHz in $CDCl_3$ and chemical shift were recorded in ppm relative to TMS. UV-visible spectra were recorded on a Shimadzu UV 1800 spectrophotometer using a 10 mm path length quartz cuvette with the wavelength in the range of 200–800 nm. Mass spectra were recorded on a Waters mass spectrometer using mixed solvent methanol and triple distilled water which was equipped with an ESI source. The pH measurements carried out using a digital pH meter (Merck). Both receptor **L** (1×10^{-5} M) and metal ions (1×10^{-4} M) solutions were prepared in CH_3CN–H_2O (1/1, v/v) and H_2O respectively.

Synthesis and characterization of L

The synthetic route of **L** has been illustrated in Scheme 1. 4-(4-Aminobenzyl)benzenamine (0.198 g, 1 mmol) was dissolved in 30 mL of dehydrated methanol, and to this, 20 mL methanol solution of 4-(diethylamino)-2hydroxybenzaldehyde (0.386 g, 2 mmol) was added drop-wise over 10 min. The reaction mixture was refluxed for 6 h at 70 °C, maintaining dry condition. A yellow precipitate was filtered and washed several times with *n*-hexane and then re-crystallized from methanol and dried in vacuum to obtain the pure yellow solid. Yield: 0.410 g (75%). mp 190 °C; anal. calc. for $C_{35}H_{40}N_4O_2$: C, 76.57 (76.62%); H, 7.38 (7.35%); N, 10.25 (10.21%). ESI-MS: *m*/*z* 549.30 (MH^+, 90%, Th. value 548.32) (Fig. S1†). FTIR/cm^{-1} (KBr): 33 356(w), 2966(s), 2913(m), 2670(w), 1638(vs), 1568(vs), 1516(vs), 1419(s), 1351(s), 1290(m), 1221(m), 1134(m), 1064(m), 1004(m), 977(m), 882(s), 821(vs), 779(vs), 701(s), 639(s), 568(s), 535(m), 448(w) (Fig. S2†).^{1}H NMR (400 MHz, $CDCl_3$, TMS): δ 13.88 (s, 1H, –OH),

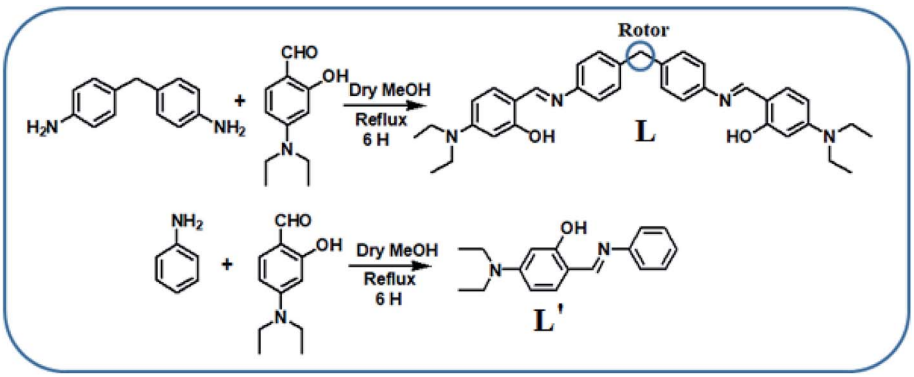

Scheme 1 Synthetic procedure of L.

8.40 (s, 1H, –CH=N), 7.13–7–20 (m, 5H), 6.24 (d, 1H), 6.19 (s, 1H), 3.99 (s, 1H), 3.39 (m, 4H), 1.21 (t, 6H) (Fig. S3†). UV-Vis λ_{max}/nm (ε/dm^3 mol^{-1} cm^{-1}) (CH_3CN): 380 (4980).

Synthesis of 5-(diethylamino)-2-((phenylimino)methyl)phenol (L′)

This was prepared by following reported procedures.[22,23] Freshly distilled aniline (0.93 g, 10 mmol) in dry methanol (20 mL) was slowly added to a well stirred solution of 4-(diethylamino)salicylaldehyde (1.93 g, 10 mmol) in dry methanol (40 mL), and the resulting orange yellow solution was stirred for a further 3 h. The reaction mixture was concentrated *in vacuo*, the residue was purified by flash SiO_2 column chromatography eluting with hexane/AcOEt. Orange yellow crystalline compound were filtered off, washed with cold methanol, then recrystallized from ethanol to give orange single crystals. Yield, 2.15 g (80%), mp 91–92 °C. Anal. calcd for $C_{17}H_{20}N_2O$: C, 76.09 (76.15%); H, 7.51 (7.47%); N, 10.44 (10.51%).

UV-Vis titration

A stock solution of **L** (1×10^{-3} M) was prepared by dissolving 5.48 mg in 10 mL of mixed solvent CH_3CN–H_2O (1/1, v/v). 30 μL of this solution were then diluted with 2.97 mL of solvent mixture to make a final concentration of 10 μM. Stock solution of Al^{3+} was prepared by dissolving $Al(NO_3)_3$ (37.5 mg, 0.1 mM) in triple distilled water (10 mL) and 1.5–90 μL of this Al^{3+} solution (1 mM) was transferred to each receptor solution **L** (10 μM). After mixing them for a few seconds, UV-Vis spectra were recorded at room temperature.

The same procedure was followed for Fe^{3+} and Cr^{3+} using the solvent mixture CH_3CN–H_2O (1/1, v/v).

Job plot measurements

L (5.48 mg, 0.01 mM) was dissolved in 10 mL of mixed solvent CH_3CN–H_2O (1/1, v/v) to make a solution conc. of 1×10^{-3} M. From this stock solution, 100, 90, 80, 70, 60, 50, 40, 30, 20, 10 and 0 μL of the **L** solution were taken and transferred to each vials. For Al^{3+}, $Al(NO_3)_3$ (37.5 mg, 0.01 mM) was dissolved in triple distilled water. 0, 10, 20, 30, 40, 50, 60, 70, 80, 90 and 100 μL of the Al^{3+} solution were added to each diluted **L** solution in such a manner that the sum of ligand and metal ion volume remains constant (3 mL) and CH_3CN–H_2O used as solvent. After mixing them for a minute, UV-Vis spectra were taken at room temperature.

The same procedure was followed for both Fe^{3+} and Cr^{3+} using the solvent mixture CH_3CN–H_2O (1/1, v/v).

Competition with other metal ions

To determine the possible interference from other metal ions and selective binding affinity of chemo sensor **L** towards Al^{3+}, Fe^{3+} and Cr^{3+}, UV-Vis spectra were taken in presence of other analytes. Stock solution of 1×10^{-3} M was prepared for receptor **L**. 30 μL of it was diluted to 3 mL with the solvent mixture to make a final concentration of 10 μM. 10 mM stock solution for various metal ions Co^{2+}, Ni^{2+}, Cu^{2+}, Ag^{+}, Zn^{2+}, Cd^{2+}, Ca^{2+}, Mn^{2+}, Mg^{2+}, Ga^{3+}, Co^{3+}, Ru^{3+}, Cr^{6+}, Na^{+}, K^{+}, Hg^{2+}, Fe^{2+}, Ba^{2+} and Pb^{2+} were prepared in triple distilled water. Each $M(NO_3)_x$ (0.1 mmol) (where, M = Al^{3+}, Fe^{3+} and Cr^{3+}) were dissolved in 10 mL of triple distilled water. After that 30 μL of each metal solution was taken from the stock and added to 3 mL of receptor **L** (10 μM) to maintain 10 equiv. of mixed solutions. Then, 30 μL of M solution (10 mM) (where, Al^{3+}, Fe^{3+} and Cr^{3+}) were added to the mixed solution of each metal ion and **L** to make a total of 10 equiv. After mixing them for seconds, UV-Vis spectra were obtained at room temperature.

pH effect test

A series of buffers with pH values ranging from 2 to 11 was prepared using 100 mM HEPES buffer. Ligand **L** (5.48 mg, 0.01 mmol) was dissolved in 10 mL of solvent mixture CH_3CN–H_2O (1/1, v/v) and when the desired pH was achieved, then 30 μL of this stock receptor solution (1 mM) was diluted to 3 mL with the abovementioned buffers to make the final concentration of 10 μM. 37.5 g $Al(NO_3)_3$ was dissolved in 10 mL HEPES buffer to maintain pH 7. Then 30 μL of this Al^{3+} solution (10 mM) was transferred to each receptor solution (10 μM) prepared above. After mixing them for a few seconds, UV-Vis spectra were taken at room temperature.

The same procedure was followed for both Fe^{3+} and Cr^{3+} using the solvent mixture CH_3CN–H_2O (1/1, v/v).

Colorimetric test kit

1 mM solution of **L** was prepared by dissolving 5.48 mg in 10 mL acetonitrile–H_2O. Test kits were obtained by immersing filter-papers into this 1 mM solution and then dried in air to get rid of the solvent. Nitrate salts of Co^{2+}, Ni^{2+}, Cu^{2+}, Ag^{+}, Zn^{2+}, Cd^{2+}, Ca^{2+}, Mg^{2+}, Ga^{3+}, Co^{3+}, Ru^{3+}, Cr^{6+}, Na^{+}, K^{+}, Hg^{2+}, Fe^{2+}, Ba^{2+}, Al^{3+}, Fe^{3+}, Cr^{3+}, Pb^{2+} and sulphate salt of Mn^{2+} were dissolved in water (10 mL) to prepare 0.1 mM solution. The above test kits were dipped into the aqueous solution of different cations solutions and then dried at room temperature to observe the colour change.

Theoretical calculation methods

The GAUSSIAN-09 Revision C.01 program package was used for all calculations.[24] The gas phase geometries of the compound was fully optimized without any symmetry restrictions in singlet ground state with the gradient-corrected DFT level coupled with the hybrid exchange–correlation functional that uses Coulomb-attenuating method B3LYP.[25] Basis set 6-31++G was found to be suitable for the whole molecule. LanL2DZ basis sets were implemented for the geometry optimization of **L** + M^{3+} complexes (M = Al, Cr and Fe).

Results and discussion

Synthesis and structure of L

The receptor **L** was synthesized in one single pot with 75% yield *via* Schiff base condensation reaction of 4-(4-aminobenzyl) benzenamine with 4-(diethylamino)-2-hydroxybenzaldehyde (Scheme 1). Then synthesized **L** was characterized by UV-Vis, FTIR, ^{1}H NMR, elemental analysis, and ESI-mass

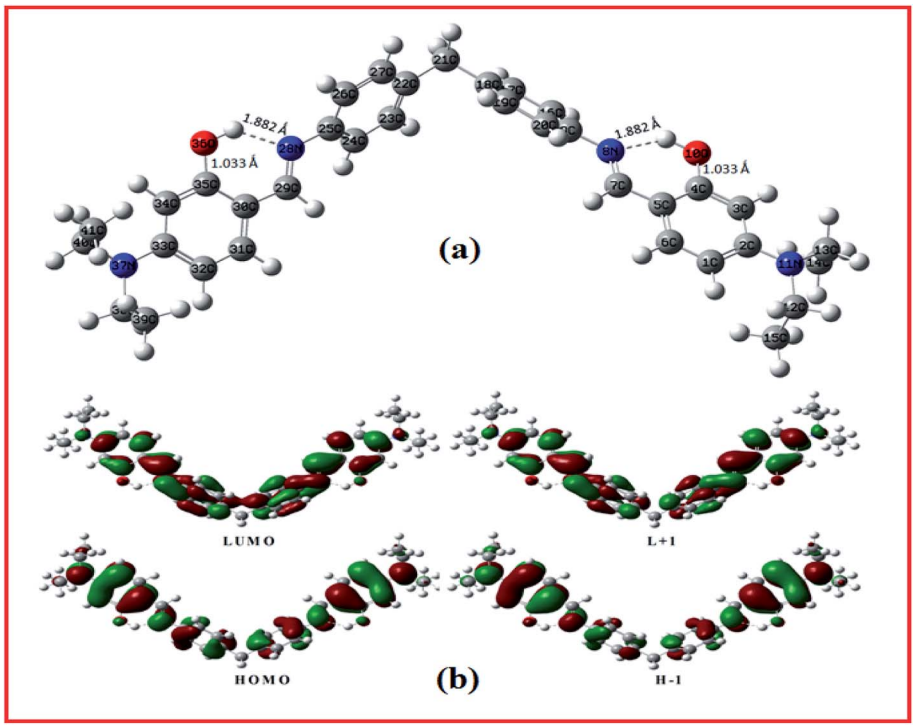

Fig. 1 (a) Geometry optimized diagram of the molecule L; (b) the contour diagrams of selected HOMO and LUMO orbitals of L. Positive values of the orbital contour are represented in purple (0.04 au) and negative values in green (−0.03 au).

spectrometric analysis. Here the two –OH groups are directed in *cis* fashion and are readily accessible to coordinate with metal ions.

DFT calculations were performed on the molecule **L**. The geometry optimizations staring from Gauss view structure of **L** lead to a global minimum as stationary level. The optimized structure of the **L** has been shown in Fig. 1a and its geometry optimized selected bond length and angles are tabulated in Table S1.† Fig. 1b presents a schematic representation of the contours of selected HOMO and LUMO orbitals of the receptor **L**. The HOMO to LUMO energy gap in **L** is 3.004 eV. The probe **L** in presence of M^{3+} ions (M = Al, Cr and Fe) form tetra-coordinated complexes, co-ordinating with salicylaldehyde O and imino N atoms of two ligand molecules in 2 : 2 fashion; which have further been confirmed by ESI-MS studies (*vide infra*). Energy minimized structure and frontier orbital contribution of the **L** + M^{3+} complexes (M = Al, Cr and Fe) have been shown in Fig. S4 and S5.†

UV-Vis studies

The sensing properties of receptor **L** were initially evaluated by the naked-eye and UV-Vis analysis. The absorbance spectra of different metal cations were studied in three categories. (i) Metal cations of the same period in the periodic table of elements such as Mn^{2+}, Fe^{3+}, Fe^{2+}, Co^{2+}, Ni^{2+}, Cr^{3+}, Cu^{2+}, Cr^{6+}, Co^{3+} and Zn^{2+}; (ii) some hazardous heavy metal ions such as Pb^{2+}, Hg^{2+}, Cd^{2+}, Ag^{+}; and (iii) a few metal cations in the IA, IIA and IIIA groups such as Na^{+}, K^{+}, Ba^{2+}, Ca^{2+}, Mg^{2+}, Ga^{3+}, and Al^{3+} in CH_3CN–H_2O (1 : 1, v/v) mixture. The receptor **L** showed small absorption bands at 271 nm due to the conjugated π–π* transition and an intense band centered at 380 nm due to n–π* transition and intra-molecular charge transfer respectively. Upon the addition of 1 equiv. of each metal ion to the receptor only Al^{3+}, Fe^{3+} and Cr^{3+} ions showed a red shifted band at 422 nm, 422 nm and 416 nm respectively, while other metal ions exhibited no changes in the absorption spectra relative to the free receptor (Fig. 2). For Cu^{2+} ion, slightly red shift in the spectral position at 380 nm was observed with negligible colour change visualized through naked eyes. Consistent with the change of the UV-Vis spectrum, colour of the solution changed from colourless to orange yellow for $Al^{3+}$and Fe^{3+} ions and

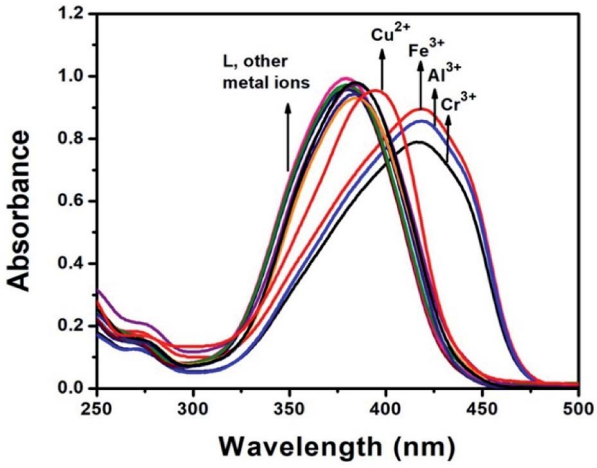

Fig. 2 Absorbance spectral change of the receptor L (10 μM) in the presence of 1 equiv. of various metal ions in CH_3CN–H_2O (1/1, v/v) solvent mixture.

Fig. 3 The colour changes of L (10 μM) upon addition of various metal ions (1 equiv.) in $CH_3CN–H_2O$ (1 : 1, v/v) at room temperature.

colourless to light yellow for Cr^{3+} ion (Fig. 3). The bar graph, showing relative absorbance intensity has been shown in Fig. S6.† The colour and spectral change can be explained by intramolecular charge transfer (ICT) and ligand-to-metal charge-transfer (LMCT) mechanisms. The red shift in the absorption band indicated that the energy gap of ICT band decreases, upon binding of metal ions to the electron withdrawing imine moieties and showed color in visible region in comparison to other metal ions. The molar extinction coefficient was calculated to 4.2×10^3, 4.4×10^3 and 3.9×10^3 respectively at wavelength 422 nm, 422 nm and 416 nm for Al^{3+}, Fe^{3+} and Cr^{3+}, which were too large to be metal based d–d transitions and thus might be assigned as ligand to metal charge transfer (LMCT) transitions.

Table 1 Absorption properties of L in various solvents

Solvent	Wavelength in nm (λ_{max})	Molar extinction coefficient (log ε)
DMSO	387	5.04
DCM	381	5.07
DMF	384	5.06
CH_3CN	380	4.98
MeOH	377	4.92

In order to confirm the ICT property of the chemosensor, the absorbance properties of **L** were further studied in different solvents such as dimethyl-sulfoxide, *N*,*N*-dimethyl formamide, acetonitrile, methanol and dichloromethanes it has been reported that the solvent dipole can relax the ICT excited by polar solvents.[26] As shown in Fig. S7† and summarized in Table 1, the absorption spectra of **L** featured a marginal red-shift of absorption maxima with increasing solvent polarity, signifying an apparent solvent dependence of the absorption band. The chemosensor **L** exhibited solvate-chromism due to occurrence of the ICT transition in receptor **L**.

To understand the binding property of **L** with Al^{3+}, Fe^{3+} and Cr^{3+}, UV-Vis titration experiments of **L** with Al^{3+}, Fe^{3+} and Cr^{3+} were carried out. The probe **L** shows that the absorption band at 380 nm significantly decreased and absorption intensity at 422 nm, 422 nm and 416 nm monotonically increased upon gradual addition of Al^{3+}, Fe^{3+} and Cr^{3+} respectively up to 1 equiv. In case of Al^{3+} and Fe^{3+}, two isosbestic points were observed at 285 and 401 nm, but in case of Cr^{3+}, only one isosbestic point was observed at 402 nm (Fig. 4) indicating that two products were generated from **L** upon binding to Al^{3+}, Fe^{3+} and only one product was generated from **L** upon binding with Cr^{3+}. The Job's plot for the binding between **L** and Al^{3+}, Fe^{3+} and Cr^{3+} exhibited 1 : 1 or 2 : 2 stoichiometry for the **L**–Al^{3+}, **L**–Fe^{3+} and **L**–Cr^{3+}complex formation (Fig. S8†). In addition, the formation of the 2 : 2 complex for **L**–Al^{3+}, **L**–$Fe^{3+}$and **L**–Cr^{3+} were confirmed by ESI-mass spectrometry (Fig. S9†). In the positive-ion mass spectrum, the *m*/*z* peaks at 574.12, 603.42 and 599.12 were assignable to 2**L** + $2Al^{3+}$, 2**L** + $2Fe^{3+}$ and 2**L** + $2Cr^{3+}$complexes respectively. Theoretical *m*/*z* values of the proposed complexes, 2**L** + $2Al^{3+}$, 2**L** + $2Fe^{3+}$ and 2**L** + $2Cr^{3+}$ are 574.12, 603.42 and 599.12 respectively.

Based on the Job plot and ESI-mass spectrometry analysis, a 2 : 2 complex structure of **L** with Al^{3+}, Fe^{3+} and $Cr^{3+}$was proposed. The binding constants for the formation of the **L**–Al^{3+}, **L**–Fe^{3+} and **L**–Cr^{3+} complex were also calculated on the basis of the change in absorbance at 422 nm, 422 nm and 416 nm respectively by considering 2 : 2 binding stoichiometry. The binding constant (*K*) determined by using Bensei–Hildebrand method was found to be 2.9×10^4 M^{-1} for Al^{3+}, 1.079×10^5 M^{-1} for $Fe^{3+}$and 1.366×10^5 M^{-1} for Cr^{3+} respectively (Fig. S10†). The values are within those (10^3–10^7) previously reported for these trivalent cations.[1,27] The detection limit for the **L**–Al^{3+}, **L**–Fe^{3+} and **L**–Cr^{3+} complexes were determined to be 2.8×10^{-7} M, 1.9×10^{-7} M and 2.5×10^{-7} M respectively on the basis of $3\sigma/K$ (Fig. S11†). Notably, the detection limit of **L** is much lower than WHO limit,[1] suggesting that **L** could be an effective sensing material for the detection of aluminum and iron in drinking water.

To further evaluate the practical applicability of receptor **L** as an Al^{3+}, Fe^{3+} and Cr^{3+} selectivity sensor, competitive experiments were performed with different metal ions in $CH_3CN–H_2O$ (1 : 1, v/v) mixed solvent (Fig. 5, S12 and S13† respectively). The other tested cations showed relatively negligible spectral change and color change apart from some dilution effect. In the presence of other competitive cations, the **L** + Al,[3] **L** + Fe^{3+} and **L** + Cr^{3+} complex solutions offer similar absorption profile. Thus, **L** could be utilized as a selective colorimetric sensor for Al^{3+}, Fe^{3+} and Cr^{3+} in the presence of other competing metal ions.

Binding mechanism

For better understanding the binding nature of **L** with Al^{3+}, Fe^{3+} and Cr^{3+}ions, ^{1}H-NMR spectra was recorded with and without these metal ions separately in DMSO–D_2O mixture. The free receptor showed chemical shifts δ at 13.88 ppm and 8.40 ppm

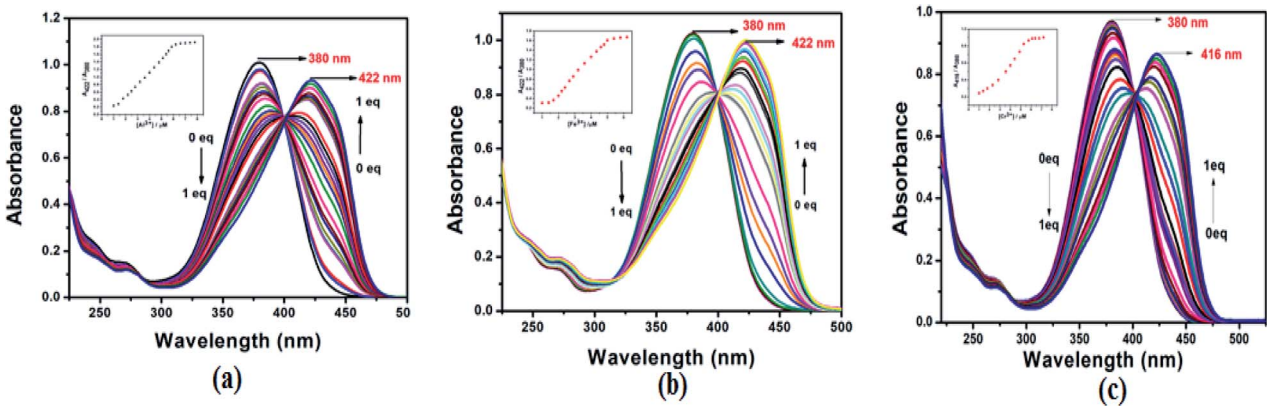

Fig. 4 Absorption spectra change of L (10 μM) in the presence of different concentrations of (a) Al^{3+}, (b) Fe^{3+} and (c) Cr^{3+} (from 0 to 1 equiv.) at room temperature. Inset: ratiometric calibration curve A_{416}/A_{380} as function of M^{3+} concentration.

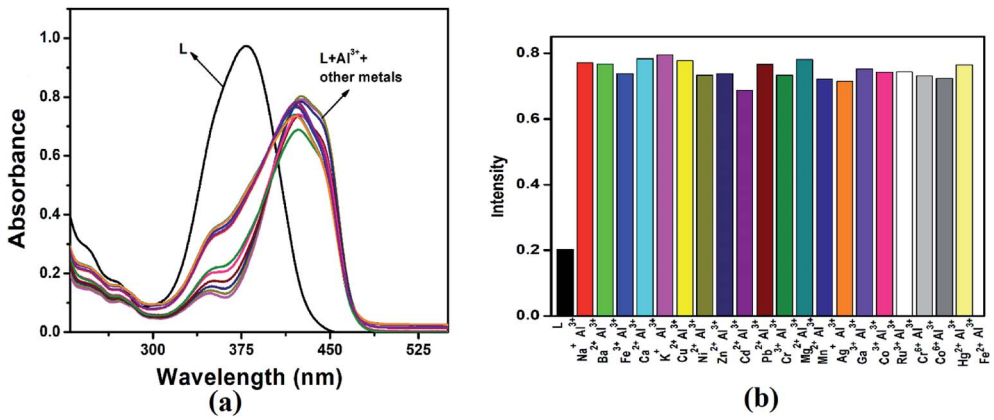

Fig. 5 Competitive selectivity of L towards Al^{3+} in the presence of other metal ions (5 equiv.) (a) absorbance spectra, (b) bar diagram taking absorption intensity at 422 nm in CH_3CN/H_2O (1/1, v/v) solution.

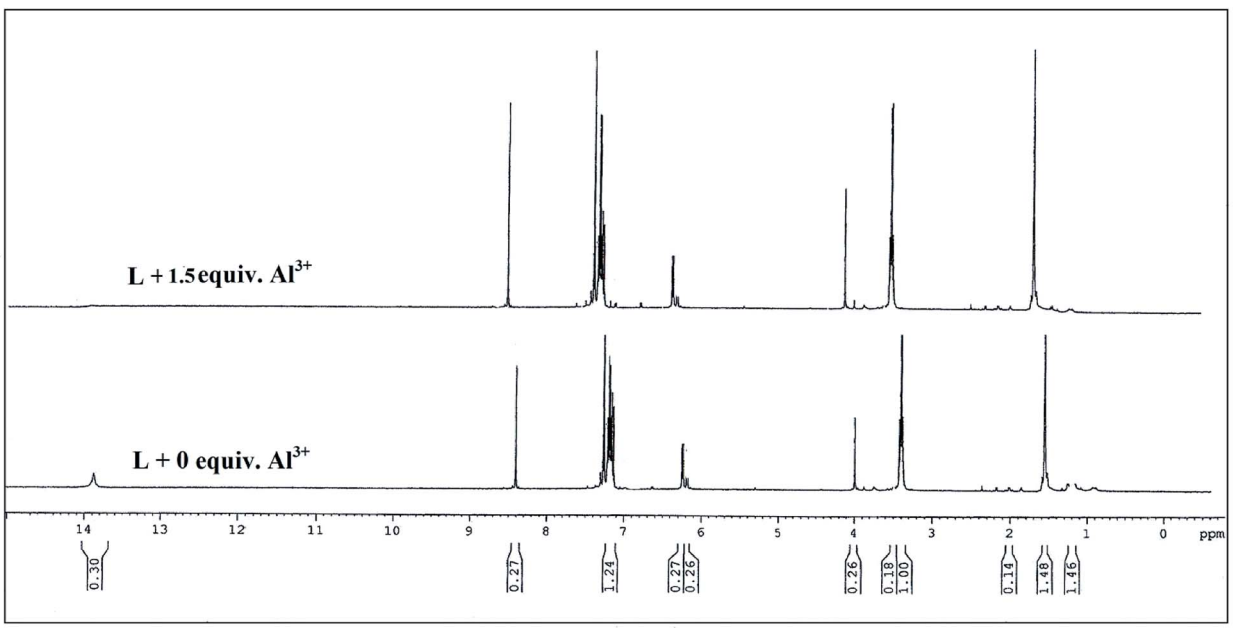

Fig. 6 ^1H NMR spectra of L in presence and absence of 1.5 equiv. Al^{3+}.

due to phenolic proton and azomethine proton respectively. Upon binding with Al^{3+}, the chemical shift at 13.88 ppm disappeared because of deprotonation of phenolic groups (Fig. 6). The other proton shift at higher δ values attributed to ligand to metal charge transfer along with intensity of the peak somewhat increased in case of M–**L** complex. Overall changes in the chemical shifts of the protons after the addition of 1.5 equiv. of Al^{3+} ion clearly reveals that the aldimine nitrogen (–CH=N) and –OH of **L** taking part in the complexation process. The most probable reason for this observation is due to the formation of symmetrical dinuclear/dimeric complex of two ligands with two metal ions (Fig. 7). Further the ESI-MS of host–guest complex confirmed the 2 : 2 binding stoichiometry (Fig. S8†).

Another indirect approach has also been made to confirm the 2 : 2 binding of **L** with Al^{3+}, Fe^{3+} and Cr^{3+} ions. The colorimetric investigations were performed using alternative Schiff base (**L′**), a monodentate version of **L**, generated from simple aniline and 4-(diethylamino)-2-hydroxybenzaldehyde under similar experimental condition. Among the mentioned ions an intense absorption band around 418 nm of receptor **L′** in CH_3CN–H_2O (1/1, v/v) decreased and a new band at 352 nm arose only in presence of Cu^{2+} ion with obvious color change from yellow to colorless. The absorption titration experiment also confirms the color and spectral changes in presence of Cu^{2+} (Fig. 8). At the same time, monodentate imine chemosensor **L′** has no influence on the target ions Al^{3+}, Fe^{3+} and Cr^{3+} (Fig. 9). So **L′** is a Cu^{2+} ion selective sensor of detection limit, 4.0×10^{-7} M

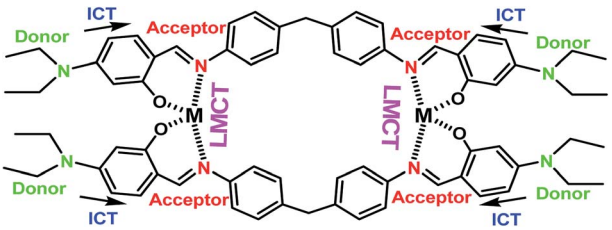

Fig. 7 Binding mechanism of L with M (M = Al^{3+}, $Fe^{3+}$and Cr^{3+}).

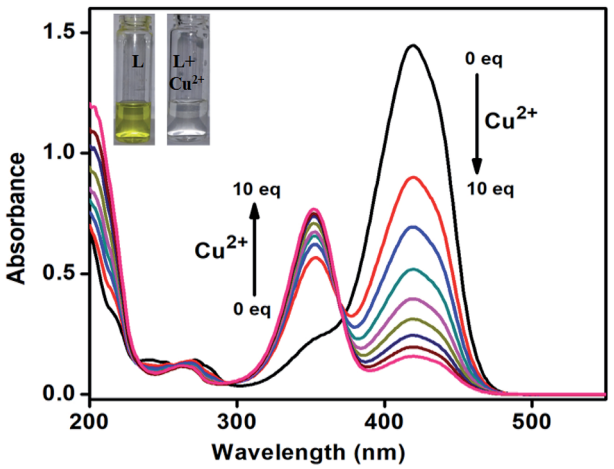

Fig. 8 Absorption titration of L′ after increasing amount of Cu^{2+}, 0–10 equiv. in CH_3CN/H_2O (1/1, v/v) solution.

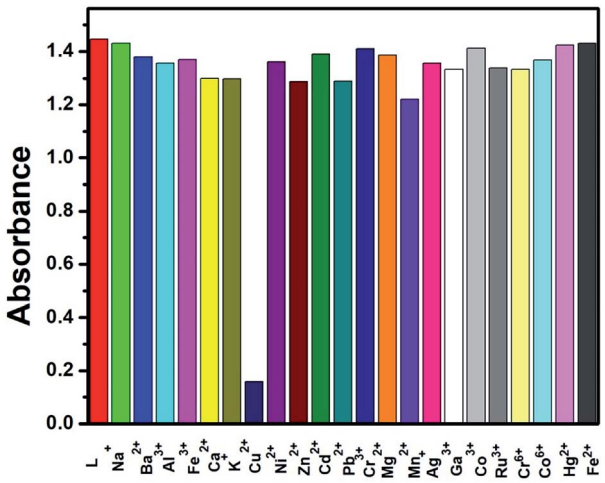

Fig. 9 Competitive selectivity of L′ towards Cu^{2+} in the presence of other metal ions.

and stability constant, 1.35×10^5 M^{-1} (Fig. S14 and S15†). It is to be mentioned here that **L′** can also be used in detection of boronic acid derivatives in living cells.[23] Thus the methylene bridged di-aniline based receptor **L** has selective affinity towards Al^{3+}, Fe^{3+} and Cr^{3+} and there 1 : 1 binding is difficult due to large distance of two imine moiety.

pH and time dependence

It is very essential to check whether the sensor is active or not for measuring specific cations in the physiological pH range. Therefore the absorption intensity of **L** between pH 2 to 11 in absence and presence of Al^{3+}, Fe^{3+} and Cr^{3+}were measured. As shown in Fig. 10, no obvious change in absorption intensity of free **L** was observed between pH 2.0–11. In the presence of 1.0 equivalent Al^{3+}, Fe^{3+} and Cr^{3+}, **L** showed maximum absorption intensity at pH range of 5.5–7.5. The absorption intensity decreases in the acidic (pH < 5) region due to protonation of imine group of **L** and therefore reduce the chelation ability.[28] Again the decreasing absorption intensity in the basic (pH > 8) region has been explained on the basis of ICT, which hindered the complexation.[29] Hence, the absorption intensity is stable over the range of pH (4–11) and well-suitable for practical application under physiological pH conditions.

The time evolution of the receptor **L** in the presence of 1.5 equiv. of Al^{3+}, Fe^{3+} and Cr^{3+} ions in CH_3CN–H_2O (1 : 1 v/v) were also being investigated (Fig. S16†). The recognition interaction gets almost completed just after the addition of 1.5 equiv. of these metal ions and the absorbance intensity remains almost the same up to 10 min. This ensures the receptor **L** to be a sensitive sensor which can be applied in environmental analysis.

Reversibility study of the chemosensor L towards Al^{3+}, $Fe^{3+}$and Cr^{3+}

Reversibility is a prerequisite in developing novel sensor for practical application. Consequently, the chemical reversibility

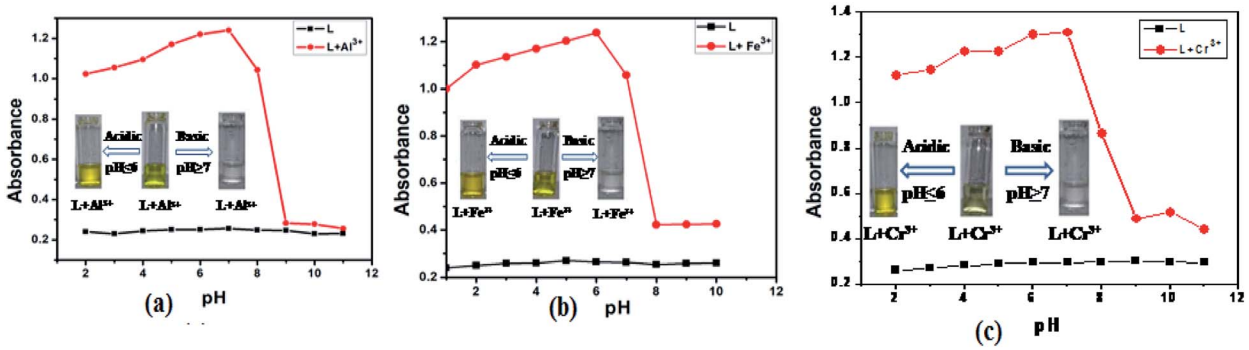

Fig. 10 Absorbance of (a) **L**, **L**–Al^{3+}, (b) **L**, **L**–$Fe^{3+}$and (c) **L**, **L**–Cr^{3+} at various ranges of pH in CH_3CN–H_2O (1 : 1, v/v) at room temperature. Inset: intensity at 422 nm, 422 nm and 416 nm respectively for **L**–M^{3+} (M = Al, Fe and Cr).

of the binding of **L** towards Al^{3+}, $Fe^{3+}$and Cr^{3+}were investigated by using different anions and disodium salt of ethylenediaminetetraacetate (Na_2EDTA). The absorption intensities of the **L**–M complexes (M = Al^{3+}, Fe^{3+} and Cr^{3+}) returned to original level upon addition of two equiv. of $NaNO_3$ (Fig. 11) solution along with the color of the solution changed back to the original colorless instantly, indicating the regeneration of the receptor **L**. Again, upon addition of Al^{3+}, Fe^{3+} and Cr^{3+} ions solution, the absorption intensity at 380 nm decreased and absorption intensity around 420 nm increased.

Moreover, the receptor **L** was applied to detect and differentiate the presence of individual Al^{3+}, $Fe^{3+}$and Cr^{3+} ions. For

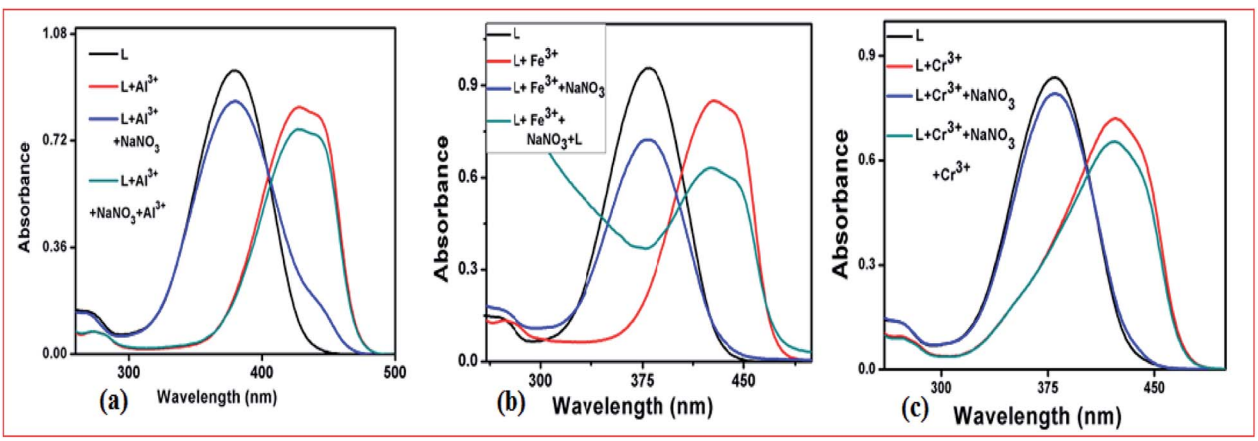

Fig. 11 Absorbance spectra of **L** in the absence and presence of (a) $Al^{3+}/NaNO_3$, (b) $Fe^{3+}/NaNO_3$ and (c) and $Cr^{3+}/NaNO_3$, respectively in CH_3CN–H_2O (1 : 1, v/v).

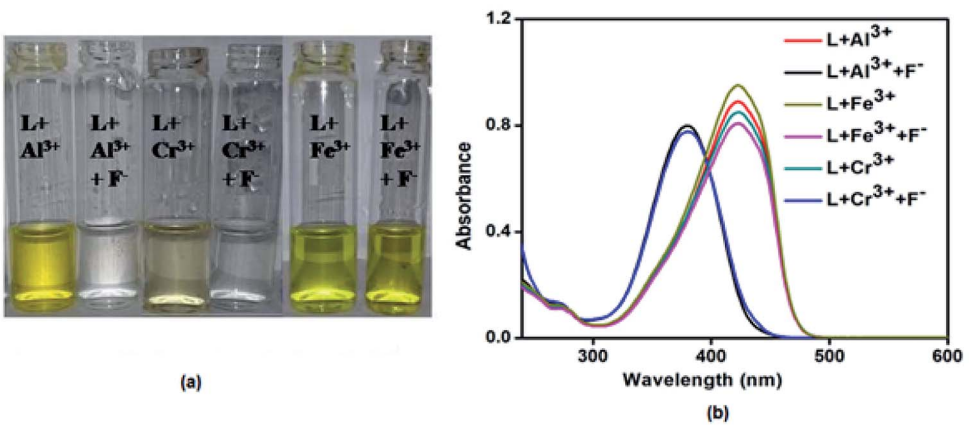

Fig. 12 Reversibility study of **L** towards Al^{3+}, $Fe^{3+}$and Cr^{3+} ions using 5 equiv. of KF (a) through color change (b) absorbance change.

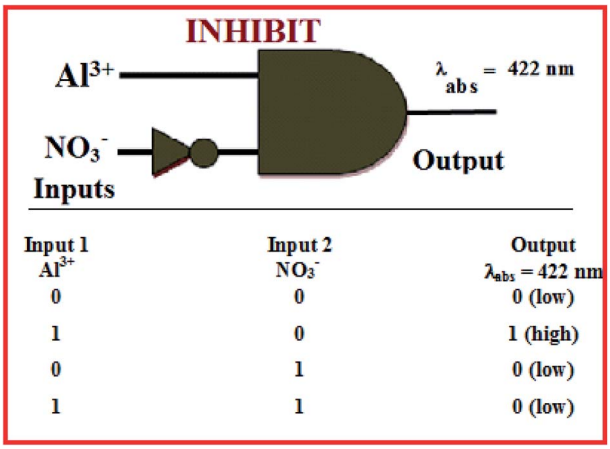

Fig. 13 Logic scheme and the truth table for the proposed INHIBIT type logic gate.

this purpose, an aqueous solution of 5 equiv. of KF was added to **L**–M adduct (M = Al^{3+}/Cr^{3+}/Fe^{3+}) solution. The color of the receptor, **L** solution containing Al^{3+} and Cr^{3+} functions as a reversible system in presence of KF whereas, it did not carry out reversibly in case of **L**–Fe^{3+}system (Fig. 12a). The same has been reflected in their UV-Vis spectra (Fig. 12b). The reversible color changes of **L** in the presence of Al^{3+} and Cr^{3+}can be explained by the higher affinity of Al^{3+} and Cr^{3+} toward F^-. Therefore, the KF solution can be used for the selective detection of Fe^{3+} in the presence of Al^{3+} and Cr^{3+} by **L**. The Al^{3+} and Cr^{3+} can be distinguished by the colour intensity, with **L**, Al^{3+} induces orange yellow colour whereas Cr^{3+} induces very light yellow colour.

If Al^{3+} and Cr^{3+} both the ions are present in the real sample then the colour of the CH_3CN–H_2O (1 : 1, v/v) solution of **L** will be intense yellow. Thus the detection of Cr^{3+} in presence of Al^{3+} in real sample is somewhat difficult. This problem can be solved by using the complexing agent cupferron, as it precipitated with both Al^{3+} and Fe^{3+} in the acidic pH and excess addition has no role towards Cr^{3+} at that condition. As the receptor **L** is also stable in the acidic pH, so no problem arises for detection of Cr^{3+} from the mixture of Al^{3+}, Fe^{3+} and Cr^{3+}.

Molecular logic gate application

The colorimetric "on–off" response of the chemosensor **L** in the presence and absence of Al^{3+} and NO_3^-, was investigated for the fabrication of a Boolean type logic gate at molecular level. The colorless solution of **L** becomes yellow only in the presence of Al^{3+} which was presented in Fig. 3, however, either NO_3^- or both Al^{3+} and NO_3^- as chemical inputs failed to produce any color change for ligand **L**. Again the change in absorbance peak at 422 nm in the absorption spectra of **L** was also being observed upon addition of Al^{3+} and NO_3^- to develop the molecular logic gate. Initially, the free receptor **L** was absorbed strongly at 380 nm in CH_3CN–H_2O (1 : 1, v/v) mixture but when Al^{3+} was added as chemical input, the absorbance peak shifted to 422 nm. Again after the addition of NO_3^- ion to the same solution it formed an un-complex system and the absorption peak of the **L** came back to its original position. Another interesting result was observed upon the addition of NO_3^- alone, where no band was observed at 422 nm. Therefore, using both the change in color and absorbance intensity at 422 nm of **L** with Al^{3+} and NO_3^- as chemical inputs which mimics the INHIBIT type logic gate at molecular level,[30] the logic scheme and truth table can be explained as shown in Fig. 13. The presence and absence of chemical inputs was assigned as 1 (on-state) and 0 (off-state) and the enhanced absorbance of **L** as 1 (on-state) and the low absorbance as 0 (off-state).

Table 2 Determination of Al^{3+}, Fe^{3+} and Cr^{3+} ions in tap water samples

Metal ion	Spiked amount (μM)	Recovered amount (μM)	% recovery ± SD (n=3)
Al^{3+}	10	9.34	93.4 ± 2.3
	20	19.60	98.0 ± 1.1
Fe^{3+}	10	10.68	106.8 ± 1.8
	20	19.47	97.35 ± 3.1
Cr^{3+}	10	9.03	90.3 ± 1.5
	20	20.69	103.45 ± 1.4

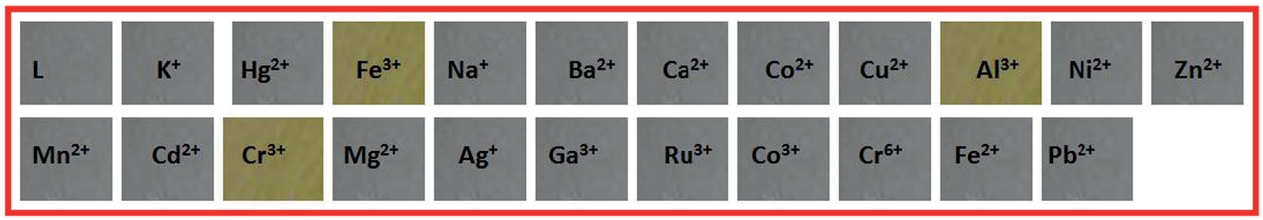

Fig. 14 Photographs of the test kits with L for detecting the Al^{3+}, Fe^{3+} and Cr^{3+} ions in acetonitrile–water solution (1 : 1, v/v) with other cations.

Table 3 Comparison of L with other colorimetric trivalent chemosensors

Probe	No. of steps involved	Solvent	LOD	K_a	Ref.
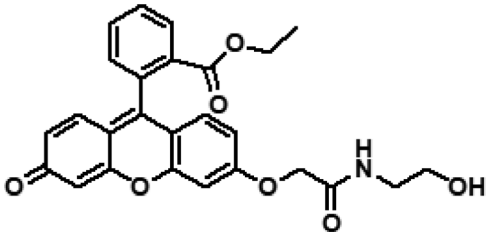	3	Pure CH_3CN	0.3 μM (Al^{3+}) 0.2 μM (Fe^{3+}) 0.5 μM (Cr^{3+})	6.46×10^9 M^{-2} (Al^{3+}) 1.26×10^5 M^{-1} (Fe^{3+}) 1.58×10^4 M^{-1} (Cr^{3+})	31
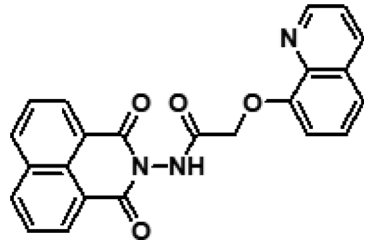	3	CH_3CN–HEPES buffer (40/60, v/v)	23 μM (Al^{3+}) 20 μM (Fe^{3+}) 25 μM (Cr^{3+})	8.77×10^3 M^{-1} (Al^{3+}) 1.08×10^4 M^{-1} (Fe^{3+}) 5.67×10^3 M^{-1} (Cr^{3+})	32
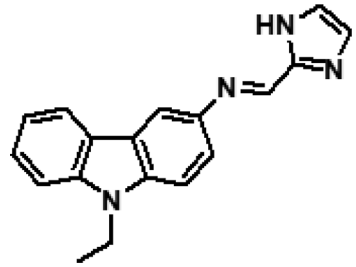	3	THF–H_2O (8 : 2)	0.38 nM (Al^{3+}) 0.38 nM (Fe^{3+}) 0.38 nM (Cr^{3+})	Not determined	33
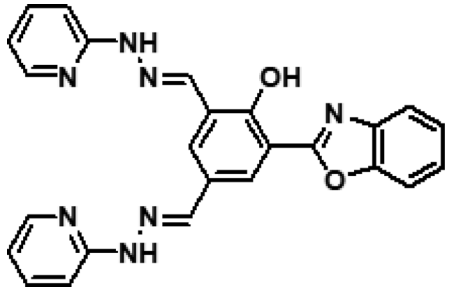	2	H_2O–EtOH (8 : 2)	0.5 μM (Al^{3+}) 0.2 μM (Cr^{3+})	2.00×10^4 M^{-1} (Al^{3+}) 5.50×10^4 M^{-1} (Cr^{3+})	34

Table 3 (*Contd.*)

Probe	No. of steps involved	Solvent	LOD	K_a	Ref.
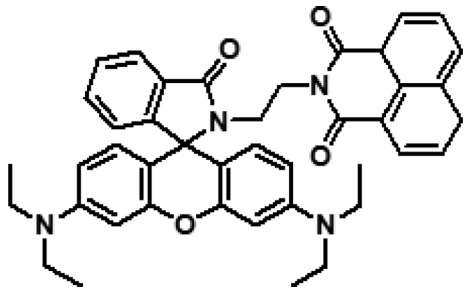	3	CH_3OH–H_2O buffer (6/4, v/v)	1.74 nM (Al^{3+}) 2.90 nM (Fe^{3+}) 2.36 nM (Cr^{3+})	1.00×10^4 M^{-1} (Al^{3+}) 1.20×10^2 M^{-1} (Fe^{3+}) 2.60×10^2 M^{-1} (Cr^{3+})	1*a*
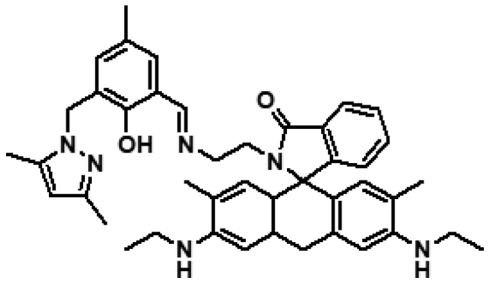	3	CH_3OH–H_2O (1/1, v/v)	0.34 μM (Al^{3+}) 0.29 μM (Fe^{3+}) 0.31 μM (Cr^{3+})	8.20×10^4 M^{-2} (Al^{3+}) 6.70×10^4 M^{-1} (Fe^{3+}) 6.00×10^4 M^{-1} (Cr^{3+})	1*b*
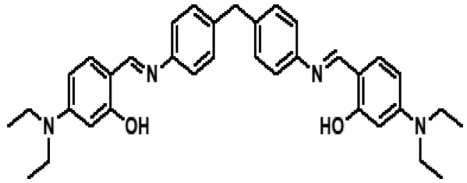	1	CH_3CN–H_2O (1/1, v/v)	0.28 μM (Al^{3+}) 0.19 μM (Fe^{3+}) 0.25 μM (Cr^{3+})	2.90×10^4 M^{-1} (Al^{3+}) 1.07×10^5 M^{-1} (Fe^{3+}) 1.36×10^5 M^{-1} (Cr^{3+})	This work

Application of chemosensor L in real samples

In order to determine the environmental application of the chemosensor **L**, artificial Al^{3+}, Fe^{3+} and Cr^{3+} contaminated different water samples have been prepared. The tap water samples were spiked with Al^{3+}, Fe^{3+} and Cr^{3+}standard solutions at different concentration levels, and then tested their concentrations with the proposed method. The percentage of recovery along with standard deviations of the spiked samples analysed by the probe **L** give satisfactory results (Table 2).

Colorimetric test-kits

To check the practical application of probe, test kits were prepared by immersing papers in a CH_3CN solution of **L** and then dried in air. These test kits were used to sense Al^{3+}, Fe^{3+} and Cr^{3+} ions among different cations. When the test kits coated with receptor **L** were added into different cation solutions, the obvious color change were observed only with Al^{3+}, Fe^{3+} and Cr^{3+} in CH_3CN–H_2O (1 : 1, v/v) solution which was shown in Fig. 14. Hence, the test kits coated with receptor **L** solution would be suitable for simultaneously detection of Al^{3+}, Fe^{3+} and Cr^{3+} by showing colors change in the presence of different metal ions.

Comparison of L with other colorimetric trivalent (Al^{3+}, Fe^{3+} and Cr^{3+}) chemosensors

The probe **L**, has been compared with some other recently reported colorimetric trivalent (Al^{3+}, Fe^{3+} and Cr^{3+}) chemosensors (Table 3). Our system has some advantages over the others. In our method, **L** has been prepared by facile, single step synthetic procedure, using inexpensive reagents without troublesome and chromatographic purification. It has very quick response time and wide linear response range. It works in CH_3CN–H_2O (1 : 1, v/v). It has fairly low detection limits and high association constants.

Conclusions

In brief, a simple colorimetric chemosensor **L** was successfully designed and synthesized for recognition of Al^{3+}, Fe^{3+} and Cr^{3+} over competing relevant metal ions in CH_3CN–H_2O (1 : 1, v/v) solvent. This colorimetric chemosensor **L** exhibited a visual color change from colorless to orange yellow upon addition of Al^{3+} and $Fe^{3+}$and colorless to yellow upon addition of Cr^{3+}. The binding abilities of the chemosensor **L** with Al^{3+}, Fe^{3+} and Cr^{3+} were established by the combined UV-Vis and ESI-MS method. The detection limit of **L** for Al^{3+} (0.28 μM), Fe^{3+} (0.196 μM) and Cr^{3+} (0.25 μM) were much lower than those set by the WHO guidelines. **L** could be successfully applied to test kits and real samples for detection of Al^{3+}, Fe^{3+} and Cr^{3+} and to build an INHIBIT type molecular logic gate. The chromophore **L** has been found to exhibit antibacterial and antifungal activity. Thus the chromophore **L** was found to be better addition in the field of chemosensors.

Conflicts of interest

There is no conflict of interest.

Acknowledgements

G. K. P. would like to thank the Department of Science and Technology and Department of Biotechnology, Government of India, New Delhi for financial support. One of the authors, RC is highly thankful to University of Grant Commission (UGC), New Delhi, India, for financial support in the form of research fellowship.

References

1 (*a*) S. Paul, A. Manna and S. Goswami, *Dalton Trans.*, 2015, **44**, 11805; (*b*) R. Alam, R. Bhowmick, A. S. M. Islam, A. Katarkar, K. Chaudhuri and M. Ali, *New J. Chem.*, 2017, **41**, 8359; (*c*) C. H. Min, S. Na, J. E. Shin, J. K. Kim, T. G. Jo and C. Kim, *New J. Chem.*, 2017, **41**, 3991; (*d*) T. Kawano, T. Kadono, T. Furuichi, S. Muto and F. Lapeyrie, *Biochem. Biophys. Res. Commun.*, 2003, **308**, 35.

2 N. E. W. Alstad, B. M. Kjelsberg, L. A. Vollestad, E. Lydersen and A. B. S. Poléo, *Environ. Pollut.*, 2005, **133**, 333.

3 R. W. Gensemer and R. C. Playle, *Crit. Rev. Environ. Sci. Technol.*, 1999, **29**, 315–450.

4 T. P. Flaten and M. Ødegård, *Food Chem. Toxicol.*, 1988, **26**, 959.

5 J. Q. Ren and H. Tian, *Sensors*, 2007, **7**, 3166.

6 R. A. Yokel, *NeuroToxicology*, 2000, **21**, 813.

7 S. Kim, J. Y. Noh, K. Y. Kim, J. H. Kim, H. K. Kang, S. W. Nam, S. H. Kim, S. Park, C. Kim and J. Kim, *Inorg. Chem.*, 2012, **51**, 3597.

8 V. K. Gupta, A. K. Jain and G. Maheshwari, *Talanta*, 2007, **72**, 1469.

9 T. P. Flaten, *Brain Res. Bull.*, 2001, **55**, 187.

10 R. B. Latmani, A. Obraztsova, M. R. Mackey, M. H. Ellisman and B. M. Tebo, *Environ. Sci. Technol.*, 2007, **41**, 214.

11 (*a*) A. K. Singh, V. K. Gupta and B. Gupta, *Anal. Chim. Acta*, 2007, **585**, 171; (*b*) J. B. Vincent, *Nutr. Rev.*, 2000, **58**, 67.

12 X. Hu, J. Chai, Y. Liu, B. Liu and B. Yang, *Spectrochim. Acta, Part A*, 2016, **153**, 505.

13 R. Crichton, *Inorganic Biochemistry of Iron Metabolism: From Molecular Mechanism to Clinical Consequences*, John Wiley & Sons Ltd, Chichester, 2nd edn, 2001, p. 326.

14 (*a*) H. Sang, P. Liang and D. Du, *J. Hazard. Mater.*, 2008, **154**, 1127; (*b*) S. J. Djane, M. Gra and C. Korn, *Spectrochim. Acta, Part B*, 2000, **55**, 389; (*c*) B. K. Datta, D. Thiyagarajan, A. Ramesh and G. Das, *Dalton Trans.*, 2015, **44**, 13093.

15 (*a*) S. Samanta, S. Goswami, A. Ramesh and G. Das, *Sens. Actuators, B*, 2014, **194**, 120; (*b*) S. Dey, S. Sarkar, D. Maity and P. Roy, *Sens. Actuators, B*, 2017, **246**, 518.

16 (*a*) X. Chen, X. Y. Shen, E. Guan, Y. Liu, A. Qin, J. Z. Sun and B. Z. Tang, *Chem. Commun.*, 2013, **49**, 1503; (*b*) N. R. Chereddy, P. Nagaraju, M. V. N. Raju, V. R. Krishnaswamy, P. S. Korrapati, P. R. Bangal and V. J. Rao, *Biosens. Bioelectron.*, 2015, **68**, 749.

17 (*a*) T. Simona, M. Shellaiah, V. Srinivasadesikan, C.-C. Lin, F.-H. Ko, K. W. Sun and M.-C. Lin, *Sens. Actuators, B*, 2016, **231**, 18; (*b*) A. Singh, R. Singh, M. Shellaiah, E. C. Prakash, H.-C. Chang, P. Raghunath, M.-C. Lin and H.-C. Lin, *Sens. Actuators, B*, 2015, **207**, 338.

18 (*a*) P. N. Borase, P. B. Thale, S. K. Sahoo and G. S. Shankarling, *Sens. Actuators, B*, 2015, **215**, 451; (*b*) M. Shellaiah, T. Simon, V. Srinivasadesikan, C.-M. Lin, K. W. Sun, F.-H. Ko, M.-C. Lin and H.-C. Lin, *J. Mater. Chem. C*, 2016, **4**, 2056.

19 (*a*) A. Liu, L. Yang, Z. Zhang and D. Xu, *Dyes Pigm.*, 2013, **99**, 472; (*b*) A. Ghorai, J. Mondal, S. Chowdhury and G. K. Patra, *Dalton Trans.*, 2016, **45**, 11540; (*c*) J. Wang, Y. Li, N. G. Patel, G. Zhang, D. Zhoub and Y. Pang, *Chem. Commun.*, 2014, **50**, 12258.

20 J. Miao, L. Wang, W. Dou, X. L. Tang, Y. Yan and W. S. Liu, *Org. Lett.*, 2007, **9**, 4567.

21 (*a*) A. Ghorai, J. Mondal, R. Chandra and G. K. Patra, *Dalton Trans.*, 2016, **44**, 13261; (*b*) A. Ghorai, J. Mondal, S. Bhattacharya and G. K. Patra, *Anal. Methods*, 2015, **7**, 10385; (*c*) A. Ghorai, J. Mondal, R. Chandra and G. K. Patra, *RSC Adv.*, 2016, **6**, 72185; (*d*) J. Mondal, A. K. Manna and G. K. Patra, *Inorg. Chim. Acta*, 2018, **474**, 22; (*e*) A. K. Manna, J. Mondal, R. Chandra, K. Rout and G. K. Patra, *J. Photochem. Photobiol., A*, 2018, **356**, 477.

22 G. P. Moloney, R. B. Gable, M. N. Iskander, D. J. Craik and M. F. Mackay, *Aust. J. Chem.*, 1990, **43**, 99.

23 Y. Hattori, M. Ishimura, Y. Ohta, H. Takenaka, T. Watanabe, H. Tanaka, K. Onob and M. Kirihata, *Org. Biomol. Chem.*, 2015, **13**, 6927.

24 M. J. Frisch, G. W. Trucks, H. B. Schlegel, G. E. Scuseria, M. A. Robb, J. R. Cheeseman, G. Scalmani, V. Barone, B. Mennucci, G. A. Petersson, H. Nakatsuji, M. Caricato, X. Li, H. P. Hratchian, A. F. Izmaylov, J. Bloino, G. Zheng, J. L. Sonnenberg, M. Hada, M. Ehara, K. Toyota, R. Fukuda, J. Hasegawa, M. Ishida, T. Nakajima, Y. Honda, O. Kitao, H. Nakai, T. Vreven, J. A. Montgomery Jr, J. E. Peralta, F. Ogliaro, M. Bearpark, J. J. Heyd, E. Brothers, K. N. Kudin, V. N. Staroverov, R. Kobayashi, J. Normand, K. Raghavachari, A. Rendel, J. C. Burant, S. S. Iyengar, J. Tomasi, M. Cossi, N. Rega, J. M. Millam, M. Klene, J. E. Knox, J. B. Cross, V. Bakken, C. Adamo, J. Jaramillo, R. Gomperts, R. E. Stratmann, O. Yazyev, A. J. Austin, R. Cammi, C. Pomelli, J. W. Ochterski, R. L. Martin, K. Morokuma, V. G. Zakrzewski, G. A. Voth, P. Salvador, J. J. Dannenberg., S. Dapprich, A. D. Daniels, Ö. Farkas, J. B. Foresman, J. V. Ortiz, J. Cioslowski and D. J. Fox, *Gaussian 09, Revision C.01*, Gaussian Inc., Wallingford, CT, 2009.

25 (*a*) A. D. Becke, *J. Chem. Phys.*, 1993, **98**, 5648; (*b*) C. Lee, W. Yang and R. G. Parr, *Phys. Rev. [Sect.] B*, 1988, **37**, 785.

26 (*a*) K. C. Song, H. Kim, K. M Lee, Y. S Lee, Y. Do and M. H. Lee, *Sens. Actuators, B*, 2013, **176**, 850; (*b*) S. Maruyama, K. Kikuchi, T. Hirano, Y. Urano and T. Nagano, *J. Am. Chem. Soc.*, 2002, **124**, 10650; (*c*) A. P. Silva, H. Q. N. Gunaratne, T. Gunnlaugsson, A. J. M. Huxley, C. P. McCoy, J. T. Rademacher and T. E. Rice, *Chem. Rev.*, 1997, **97**, 1515.

27 (*a*) S. Goswami, K. Aich, S. Das, A. K. Das, D. Sarkar, S. Panja, T. K. Mondal and S. Mukhopadhyay, *Chem. Commun.*, 2013, **49**, 10739; (*b*) A. Barba-Bon, L. Calabuig, A. M. Costero, S. Gil, R. Martínez-Máñez and F. Saneńona, *RSC Adv.*, 2014, **4**, 8962.

28 L. Wang, W. Qin, X. Tang, W. Dou, W. Liu, Q. Teng and X. Yao, *Org. Biomol. Chem.*, 2010, **8**, 3751.

29 A. Banerjee, A. Sahana, S. Das, S. Lohar, S. Guha, B. Sarkar, S. K. Mukhopadhyay, A. K. Mukherjee and D. Das, *Analyst*, 2012, **137**, 2166.

30 D. Sarkar, A. Pramanik, S. Biswas, P. Karmakar and T. K. Mondal, *RSC Adv.*, 2014, **4**, 30666.

31 A. Barba-Bon, A. M. Costero, S. Gil, M. Parra, J. Soto, R. Martínez-Máñez and F. Sancenón, *Chem. Commun.*, 2012, **48**, 3000.

32 S. Goswami, K. Aich, A. K. Das, A. Manna and S. Das, *RSC Adv.*, 2013, **3**, 2412.

33 M. Venkateswarulu, T. Mukherjee, S. Mukherjee and R. R. Koner, *Dalton Trans.*, 2014, **43**, 5269.

34 J. Wang, Y. Li, N. G. Patel, G. Zhang, D. Zhou and Y. Pang, *Chem. Commun.*, 2014, **50**, 12258.

